RESEARCH ARTICLE

Quantitative proteomic identification of host factors involved in the *Salmonella typhimurium* infection cycle

Mijke W. Vogels[1,2], Bas W. M. van Balkom[3,4], Albert J. R. Heck[3], Cornelis A. M. de Haan[2], Peter J. M. Rottier[2], Joseph J. Batenburg[1], Dora V. Kaloyanova[1] and J. Bernd Helms[1]*

[1] Department of Biochemistry and Cell Biology, Biochemistry Division, Faculty of Veterinary Medicine, Utrecht University, Utrecht, The Netherlands
[2] Department of Infectious Diseases and Immunology, Virology Division, Faculty of Veterinary Medicine, Utrecht University, Utrecht, The Netherlands
[3] Biomolecular Mass Spectrometry and Proteomics, Bijvoet Centre for Biomolecular Research and Utrecht Institute for Pharmaceutical Sciences, Utrecht University, Utrecht, The Netherlands
[4] Department of Nephrology and Hypertension, University Medical Center Utrecht, Utrecht, The Netherlands

Received: April 28, 2011
Revised: August 25, 2011
Accepted: August 30, 2011

To identify host factors involved in *Salmonella* replication, SILAC-based quantitative proteomics was used to investigate the interactions of *Salmonella typhimurium* with the secretory pathway in human epithelial cells. Protein profiles of Golgi-enriched fractions isolated from *S. typhimurium*-infected cells were compared with those of mock-infected cells, revealing significant depletion or enrichment of 105 proteins. Proteins annotated to play a role in membrane traffic were overrepresented among the depleted proteins whereas proteins annotated to the cytoskeleton showed a diverse behavior with some proteins being enriched, others being depleted from the Golgi fraction upon *Salmonella* infection. To study the functional relevance of identified proteins in the *Salmonella* infection cycle, small interfering RNA (siRNA) experiments were performed. siRNA-mediated depletion of a selection of affected proteins identified five host factors involved in *Salmonella* infection. Depletion of peroxiredoxin-6 (PRDX6), isoform β-4c of integrin β-4 (ITGB4), isoform 1 of protein lap2 (erbin interacting protein; ERBB2IP), stomatin (STOM) or TBC domain containing protein 10b (TBC1D10B) resulted in increased *Salmonella* replication. Surprisingly, in addition to the effect on *Salmonella* replication, depletion of STOM or ITGB4 resulted in a dispersal of intracellular *Salmonella* microcolonies. It can be concluded that by using SILAC-based quantitative proteomics we were able to identify novel host cell proteins involved in the complex interplay between *Salmonella* and epithelial cells.

Keywords:
Cell biology / Host–pathogen interactions / *Salmonella typhimurium* / Secretory pathway / SILAC

Correspondence: Professor J. B. Helms, Department of Biochemistry and Cell Biology, Faculty of Veterinary Medicine, Utrecht University, Yalelaan 2, 3584 CM, Utrecht, The Netherlands
E-mail: j.b.helms@uu.nl
Fax: +31-302535492

Abbreviations: CYT, cytoskeletal protein; **ERBB2IP,** erbin interacting protein; **ITGB4,** isoform β-4c of integrin β-4; **MOI,** multiplicity of infection; **p.i.,** post-infection**PLA$_2$,** phospholipase A$_2$; **PNS,** post-nuclear supernatant; **PRDX6,** peroxiredoxin 6; **SCB,** select calcium-binding; **SCV,** *Salmonella*-containing vacuole; **siRNA,** small interfering RNA; **SPI-1,** *Salmonella*pathogenicity island 1; **STOM,** stomatin; **T3SS,** type three secretion system; **TBC1D10B,** TBC domain containing protein 10b; **wt,** wild-type

1 Introduction

Salmonella typhimurium, a Gram-negative bacterium, is a serovar of the species *Salmonella enterica*. *S. enterica* serovars cause a variety of different diseases in man and other animals. *S. typhimurium* infections are a major cause of foodborne illness in humans throughout the world. In man, *S. typhimurium* infection usually leads to a self-limiting gastroenteritis. However, in susceptible mouse strains this

*Additional corresponding author: Dr. Mijke W. Vogels
E-mail: mijke.vogels@gmail.com

bacterium provokes a typhoid-like disease, very similar to the typhoid fever caused in humans by the closely related *S. enterica* serovar *typhi* [1–3]. Investigations into host-pathogen interactions by *S. typhimurium* therefore increase not only our understanding of the pathogenesis of gastroenteritis, but also that of typhoid fever.

S. typhimurium can infect both macrophages and epithelial cells. It enters the human body by infecting microfold (M) cells, which are specialized epithelial cells in the intestinal tract, or by infecting other intestinal epithelial cells. Once the epithelial barrier has been passed, they can infect macrophages, adjacent to the epithelial layer [4, 5]. *Salmonella* can also enter the bloodstream when they are taken up by dendritic cells that are present at the basolateral side of the intestinal epithelium [6]. The infection of epithelial cells is a crucial step in *Salmonella* infection. The bacterium invades this type of cells by inducing its own uptake. For this purpose it employs a specialized secretion apparatus, called a type three secretion system (T3SS).

The *S. typhimurium* genome encodes two T3SSs that can translocate a large number of effector proteins from the bacterium into the cytosol of a host cell [7–11]. These effector proteins modify host cell functions to the benefit of the bacterium. The T3SSs are encoded by the *Salmonella* pathogenicity islands 1 and 2 (SPI-1 and SPI-2; for reviews, see [7, 8, 12–16]). To enable *Salmonella's* invasion of epithelial cells, the SPI-1-encoded T3SS of the bacterium translocates effectors across the plasma membrane of the epithelial cell. Among others, these effectors cause actin rearrangements, which induce ruffling of host cell's plasma membrane and uptake of the *Salmonella* by macropinocytosis [17–20]. Once inside the host cell, the bacterium resides in a so-called *Salmonella*-containing vacuole (SCV). The SPI-2-encoded T3SS, T3SS-2, translocates effector proteins across the membrane of the SCV into host cell's cytoplasm to promote intracellular survival and replication of *Salmonella*. In order for *Salmonella* to replicate, the SCV moves to the perinuclear region where it becomes surrounded by membranes of the Golgi apparatus. During the migration to the Golgi region, the SCV matures and recruits several markers from the endo/lysosomal system by interacting with the endocytic and secretory pathway (for extensive reviews on SCV maturation and biogenesis, see [21–26]). Three T3SS-2 effectors, SifA, SseF and SseG, were shown to be important for the maintenance of the SCV in the Golgi region [27–30]. Although there is no evidence for a direct contact between *Salmonella* and the Golgi apparatus, it has been shown that intact Golgi membranes are required for efficient *Salmonella* replication. Drug-induced disruption of the Golgi apparatus has been demonstrated to decrease *Salmonella* replication [29]. In addition to positioning itself in the Golgi region during replication, *S. typhimurium* can also redirect host secretory traffic. This results in the accumulation of exocytic cargo vesicles (post-Golgi vesicles) in close proximity of the SCV [31]. Thus, during infection, *Salmonella* interacts with the host cell secretory pathway in several ways. However, the details of these interactions and the host proteins involved are largely unknown. Insight into the interplay between *Salmonella* and the host is important for our understanding of *Salmonella* infection.

To investigate *Salmonella*–host interactions in more detail we used a quantitative proteomics approach. This approach is based on stable isotope labeling by amino acids in cell culture (SILAC), developed by Ong et al. [32]. Recently, we applied this technique to investigate interactions of coronaviruses with the host secretory pathway [33]. In the present study, we compared the protein profiles of isolated Golgi-enriched fractions from cells that were either infected with *S. typhimurium* or mock-infected.

After statistical analysis, 105 proteins were identified that were significantly changed in their abundance in the Golgi-enriched fraction upon *Salmonella* infection. By depletion of a selected subset of these proteins using small interfering RNAs (siRNAs) we identified five proteins that were found to affect *Salmonella* replication.

2 Materials and methods

2.1 Cells and bacteria

HeLa cells were grown in DMEM (Cambrex) supplemented with 10% FCS, 100 IU of penicillin/mL and 100 μg of streptomycin/mL (pen/strep); all from Life Technologies (Paisley). For the infection experiments, wild-type *S. typhimurium* strain 14028 (obtained from ATCC) was used.

2.2 *Salmonella* infection

S. typhimurium cultures were grown in Luria Bertani broth (LB; Biotrading) for 16–18 h at 37°C with continuous shaking. On the day of the experiment, bacteria from the overnight culture were diluted 33 times in LB broth and incubated for another 3.5 h to reach the exponential phase as described before [34]. To follow a synchronized population of bacteria, HeLa cells were infected with *Salmonella* at a multiplicity of infection (MOI) of 100, for 15 min at 37°C in DMEM with 10% FCS, washed thoroughly with PBS and incubated in DMEM with addition of 100 μg/mL gentamycin (Gibco) for one hour to kill all extracellular bacteria. After this incubation, the medium was replaced by DMEM with 10% FCS and 10 μg/mL gentamycin and the infection was continued for 5 or 7 h for the SILAC and siRNA experiments, respectively.

2.3 $^{13}C^{15}N$-arginine- and $^{13}C^{15}N$-lysine-labeling of HeLa cells

For the $^{13}C^{15}N$-arginine- and $^{13}C^{15}N$-lysine-labeling of HeLa cells, cells were cultured in specialized medium. DMEM lacking L-arginine and L-lysine was obtained from PAN-biotech (cat. no. P04-04510S2). For the SILAC experiments

this medium was reconstituted with either the heavy amino acids, L-arginine-$^{13}C_6^{15}N_4$ hydrochloride (Spectra Stable Isotopes, cat. no. 548ARG98) and L-lysine-$^{13}C_6^{15}N_2$ hydrochloride (Spectra Stable Isotopes, cat.no. 548LYS98) (referred to as heavy medium), or with the normal, light amino acids, L-arginine-$^{12}C_6^{14}N_4$ hydrochloride (Sigma, cat. no. A5131) and L-lysine-$^{12}C_6^{14}N_2$ hydrochloride (Sigma, cat. no. L5626) (referred to as light medium) at a final concentration of 84 and 146 mg/L for arginine and lysine, respectively. The heavy and light culture media were supplemented with dialyzed FCS (Invitrogen, cat. no. 26400-044) and pen/strep similarly as described above. Cells were passaged in fresh medium when 80–90% confluency was reached. The extent and efficiency of the stable isotope labeling of the HeLa cells were checked using MALDI-TOF-TOF analysis. As was shown previously [33], already after one passage, the incorporation of the $^{13}C^{15}N$ amino acids was complete. For practical reasons, cells that had been passaged six times in the heavy medium were used in the SILAC experiments.

2.4 SILAC experiments: *S. typhimurium* infection

The SILAC procedure, which was described by Ong et al. [32], was performed with certain adjustments as we published previously [33]. Briefly, two pools of HeLa cells were used that had been passaged six times in either the heavy or the light medium. The cells were grown in T175 flasks (Corning) until confluence was reached (approximately 3×10^7 cells per flask). Cells from eight culture flasks were used per experiment, four flasks per labeling condition. In each SILAC experiment, HeLa cells cultured either in the light or the heavy medium were infected with wt *S. typhimurium* at an MOI of 100 or mock-infected for six hours as described above. Three independent SILAC experiments were performed, two in which the HeLa cells cultured in the light medium and one in which the HeLa cells cultured in the heavy medium were infected with *Salmonella*.

2.5 SILAC experiments: isolation of a Golgi-enriched fraction

Six hours post-infection (p.i.), the *Salmonella*-infected cells were harvested in homogenization buffer (250 mM sucrose in 10 mM Tris-HCl, pH7.4) and combined in a 1:1 ratio with the mock-infected cells. A Golgi-enriched fraction was isolated from the cells using an established method [33, 35–37]. Cells were homogenized with the Balch homogenizer (gap size 9 μm). Post-nuclear supernatant (PNS) was obtained after centrifugation of the cell homogenate at 1700 rpm for 10 min at 4°C. This PNS was mixed with 62% w/w sucrose (in 10 mM Tris, pH 7.4) to obtain a 37% sucrose solution. Four ml of this solution was placed into an SW40 tube and overlaid with a 35% w/w and 29% w/w layer (approximately 5 and 4 mL respectively) of sucrose solution (in 10 mM Tris, pH 7.4). This gradient was centrifuged for 2 h and 40 min at 100 000 × *g*. Approximately, 1 mL of a Golgi-enriched fraction was collected at the 35–29% sucrose interphase. For further analysis, membranes were pelleted by centrifugation for 30 min at 100 000 × *g* at 4°C after the addition of 4 volumes of PBS to 1 volume of the Golgi-enriched fraction. Golgi-enrichment of the isolated fraction was analyzed by Western blot analysis. A fraction of the PNS or Golgi-enriched membranes corresponding to 20 μg protein was dissolved in Laemmli sample buffer containing β-mercaptoethanol and heated for 5 min at 95°C. Proteins were separated using 12% SDS-PAGE. The proteins were transferred to a PVDF membrane using the Western blot system from Bio-rad and blocked in PBS/0.05% Tween/5% dried milk (Protifar, Nutricia) for 1 hour at room temperature. Primary antibodies (p23; 1:1000 [38], or β-actin; 1:2000, Abcam) were incubated in PBS/0.05% Tween/1% dried milk for 1 h at room temperature. After washing three times with PBS/0.05% Tween, the secondary antibody (gαrpo 1:10 000) was incubated for 1 h at room temperature. After another three washing steps, bound antibodies were visualized with the ECL detection kit from Pierce.

2.6 MS

A fraction of the Golgi-enriched membranes corresponding to 80 μg protein was dissolved in Laemmli sample buffer containing 10 mM DTT and heated for 5 min at 95°C. Proteins were separated in a 12% SDS-PAGE gradient gel, fixed in 5% acetic acid/30% methanol and stained using GelCode Blue reagent (Pierce). Gel lanes were cut into 24 equally sized slices, which were subjected to in-gel trypsin digestion as described [39]. Totally, 20–80% of the supernatants obtained after the digestion was used for LC-MS/MS analysis on a ThermoFinnigan FT-ICR equipped with a 7 Tesla magnet coupled to an Agilent Series 1100 binary pump system (Agilent Technologies). Peptide mixtures were trapped on an in-house packed 5 cm × 100 μm Aqua^{TM} C18 reversed-phase column (Phenomenex) at a flow rate of 5 μL/min. Peptide separation was achieved on a 15 cm × 75 μm Aqua^{TM} C18 reversed-phase column using a gradient of 0–70% solution B (solution A = 0.1 M acetic acid; solution B = 80% v/v ACN, 0.1 M acetic acid) in 60 min at a constant flow rate of 200 nL/min.

2.7 MS data analysis

Finnigan ∗.raw files were converted into ∗.dta files using BioWorks software, version 3.1 SR1 (Thermo Electron). For this process the program was set to track the scan limits automatically and calculate for peptides with a mass from 300 to 5000 amu, automatically detecting the charge state and MS level (MS or MS/MS). The threshold was set to 100 counts. Subsequently, MASCOT generic files were

generated through in-house developed software. These files were used to search the IPI_Human 3.36 database [40] on an in-house MASCOT server [41], allowing up to 2 missed cleavages, a peptide mass tolerance of 50 ppm and a fragment mass tolerance of 0.8 Da. Peptide modifications used in the searches were carbamidomethyl on cysteine (fixed) and oxidation on methionine, tryptophan and histidine (variable). Proteins matching the criteria for at least two reliable peptides (rank 1; unique; individual score higher than 29 (1% false positive rate)), and with a protein score higher than 64 were considered as positive identified proteins. Raw data files and Mascot html result pages were loaded into the MSQuant program [42] adapted for SILAC-based quantitative analysis. All quantified peptides were checked by manual inspection of the spectra used for quantification. To identify statistically different protein abundances between samples ($p < 0.05$), data from three independent experiments were loaded into the StatQuant program for statistical analysis [43].

2.8 siRNA experiments: replication assay

Two siRNA oligos per gene (targeting two different sites within the coding region) were obtained from Ambion. Validated oligos were used that induce a guaranteed knockdown by at least 80% and are chemically modified to reduce off target effects by up to 90%. For each gene, both oligos showed the same effect on *Salmonella* replication, reflecting the specificity of the validated oligos. HeLa cells were seeded into 24-well plates and transfected with a final concentration of 20 nM siRNA (each siRNA oligo was transfected separately) using Oligofectamine (Invitrogen). Scrambled siRNAs (Ambion) and mock-transfected cells (only Oligofectamine) were used as controls in each experiment. Forty-eight hours after siRNA transfection, the cells were infected with *S. typhimurium* at an MOI of 100 as described above. For counting intracellular bacteria, HeLa cells were washed three times with PBS, lysed in PBS containing 1% Triton X-100 and 0.1% SDS for 2 min and a dilution series was plated onto LB agar as described [44]. The *Salmonella* fold increase was determined by dividing the number of colony forming units (cfu) at 8 h p.i. by the number of cfu at 1 hour p.i. Each siRNA experiment was performed in triplicate.

2.9 Quantitative real-time (RT) PCR

To validate the knockdown of the targeted genes in the siRNA experiments, mRNA levels of each gene were determined. Forty-eight hours after siRNA transfection, total RNA was isolated from the interfered cells using the TRIzol reagent (Invitrogen) and further purified using the RNeasy mini kit from Qiagen. The knockdown of the targeted genes was verified by quantitative RT-PCR using Taqman Gene Expression Assays (Applied Biosystems, CA, USA). RT-PCR reactions were performed on a LightCycler 480 system (Roche). The comparative Ct-method was used to determine the fold change for each individual gene and the housekeeping gene GAPDH was used as a reference in all experiments.

2.10 Analyzing protein pattern in uninfected and infected cells

To study the protein pattern of the affected proteins in uninfected and *Salmonella*-infected cells, PNS samples obtained from those cells were analyzed by Western Blot. HeLa cells were infected with *S. typhimurium* as described above (Section 2.2) or mock-infected. Six hours p.i., the cells were harvested and homogenized with the Balch homogenizer (gap size 9 μm). PNS was obtained after centrifugation of the cell homogenate at 1700 rpm for 10 min at 4°C. The protein concentration of the PNS samples were measured using the Bradford assay and equal amounts of infected and uninfected PNS (30 μg) were loaded on gel, transferred to a PVDF membrane and stained with the appropriate antibodies as described above (paragraph 2.5). Antibodies recognizing three of the affected proteins (STOM, TBC1D10B and PRDX6) were used (Santa Cruz Biotechnology) as well as antibodies against the Gα- and Gβ-subunits of the heterotrimeric G protein (GαGβ, Santa Cruz Biotechnology) and the housekeeping gene β-actin (Abcam).

2.11 *Salmonella* microcolony morphology

To study the *Salmonella* microcolony after siRNA-mediated depletion of the selected proteins, HeLa cells were seeded onto glass coverslips in a 24-well plate (Corning), depleted for the selected proteins as described above and infected with *S. typhimurium* at an MOI of 100. At 6 hours p.i., the cells were fixed with 3.7% paraformaldehyde (PFA) for 15 min at room temperature, washed with PBS and permeabilized and blocked by incubating with blocking buffer (BB: 2% BSA/0.1% saponin in PBS) for 30–60 min at room temperature. Subsequently, the cells were incubated with the primary antibodies targeting the Golgi marker GM130 (anti-GM130, 1:400, BD Transduction Laboratories) or the lipopolysaccharide of *Salmonella* (anti-LPS, 1:400, Abcam) in BB for 60 min at room temperature. Cells were washed thoroughly with PBS and incubated with the secondary antibodies (goat-anti-mouse or goat-anti-rabbit antibodies conjugated with Alexa dyes 488 or 568; all from Invitrogen) for another 60 min at room temperature. After this incubation step, cells were washed three times with PBS, mounted on glass slides using FluorSave reagent (Calbiochem) and analyzed on a confocal microscope (Leica TCS Sp2 CLSM). For quantification of two different microcolony phenotypes (tight and dispersed), three independent

experiments were performed in which 100 cells were counted per condition. We scored a microcolony as being dispersed when the percentage of open space within the microcolony area was higher than 75%.

3 Results

3.1 SILAC experiments

We compared the protein profiles of Golgi-enriched fractions from cells that were either infected with *S. typhimurium* or mock-infected by applying a quantitative proteomics approach, based on SILAC. Three independent experiments were performed, two in which the light cells were infected and one in which the heavy cells were infected with *Salmonella*. Since *Salmonella* replication is strongly dependent on its Golgi localization [29], which occurs 4–8 h p.i., we allowed infection to proceed for 6 h before Golgi isolation.

Six hours p.i. the *Salmonella*-infected cells were combined with the control mock-infected cells and a well-defined Golgi-enriched fraction was isolated using established procedures [33, 35–37]. Enrichment of the Golgi membranes in the isolated fractions was confirmed by Western blot analysis using antibodies recognizing the Golgi marker protein p23 (Fig. 1A).

Proteins from the isolated Golgi fractions were separated by SDS-PAGE, digested using in-gel tryptic digestion and

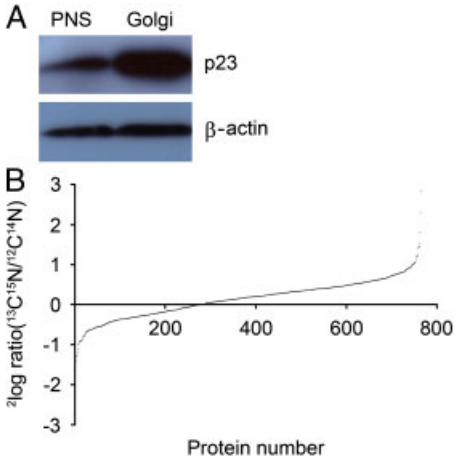

Figure 1. Ratio distribution of the identified proteins. Proteomic analysis was performed on Golgi-enriched fractions. The enrichment of Golgi membranes in the isolated fraction (lane 2, 20 μg protein) was confirmed by Western blotting using the Golgi marker protein p23 by comparison with PNS (lane 1, 20 μg protein) (A). The ratios between the 'heavy' and 'light' peak in the corresponding mass spectra of the 765 identified proteins were calculated and plotted in the ratio distribution graph (B). The ratios of the majority of the proteins distributed around 1 ($\log_2$ ratio = 0), confirming that the samples had been mixed equally and indicating that the majority of the proteins did not change in abundance upon *Salmonella* infection.

subjected to LC-MS/MS. After Mascot database screening, the identified proteins were quantified using MSQuant [42], resulting in the identification of 765 proteins (referred to as identified proteins; Supporting Information Table S1) that were reliably identified and quantified. To analyze the differential expression of the identified proteins during *Salmonella* infection, ratios of the heavy and the light peak in the corresponding mass spectra were calculated (as described in Section 2). Figure 1 shows the ratio distribution of the 765 identified proteins. For the majority of the proteins, the ratios were distributed around 1 (^{2}log ratio = 0), confirming that the *Salmonella*-infected and mock-infected cells had been mixed in equal numbers and indicating that the majority of the proteins were not changed in abundance due to the infection. The StatQuant program [43] was used to calculate for which proteins the ratios differed significantly ($p < 0.05$) from the mean. This analysis showed that the abundance of 105 proteins had significantly changed (referred to as affected proteins; Table 1) in the Golgi-enriched fraction upon infection. Of these 105 affected proteins, 50 were enriched (^{2}log ratio < 1, referred to as enriched proteins) and 55 were depleted (^{2}log ratio > 1, referred to as depleted proteins) in the isolated Golgi-enriched fraction.

3.2 Protein analysis

To gain more insight into the origin and function of the identified proteins, they were classified according to their subcellular location or molecular function annotation, using the Universal Protein Resource database (www.uniprot.org) and the PANTHER Classification System (Protein ANalysis THrough Evolutionary Relationships, http://www.pantherdb.org [45]), respectively.

In Fig. 2A the categorization of the 765 identified proteins according to subcellular location annotation is compared with the 105 affected proteins. As expected, the 765 identified proteins were distributed among several different groups, since diverse intracellular membranes are known to be present in the isolated Golgi fraction, albeit at lower abundance [36]. The overall distribution of the 105 affected proteins was only slightly different from that of the 765 identified proteins. The distribution of the affected proteins is somewhat changed for the cytoskeletal (CYT)-, Golgi apparatus-, mitochondrial- and endosomal-localized proteins. As the distribution of proteins among different organelles in Fig. 2A does not distinguish between enrichment in or depletion from the Golgi-enriched fraction upon infection, the affected proteins were analyzed in more detail for enriched and depleted proteins separately (Fig. 2B). The largest group of proteins consisted of proteins annotated to be localized to the cytoplasm. This group contained an equal proportion of enriched and depleted proteins. The proteins annotated to originate from the cytoskeleton and the Golgi apparatus were also both enriched in and/or depleted from the Golgi-enriched fraction upon infection. The affected

Table 1. List of affected proteins in Golgi-enriched fraction of *Salmonella*-infected HeLa cells relative to mock-infected cells based on SILAC analysis

ProteinID	Protein	Mean ratio[a)]	*p*-Value
Enriched proteins			
IPI00008780	Stanniocalcin-2 precursor	0.216	0.0129
IPI00410034	Solute carrier family 38 member 2	0.225	0.0096
IPI00025447	EEF1A1protein	0.498	0.0014
IPI00025512	Heat-shock protein β-1	0.499	0.0329
IPI00178440	Elongation factor 1-β	0.520	0.0167
IPI00023860	Nucleosome assembly protein 1-like 1	0.530	0.0368
IPI00001560	Isoform 1 of cyclin-dependent kinase inhibitor 2A	0.536	0.0239
IPI00217683	A-kinase anchor protein 12 isoform 2	0.545	0.0317
IPI00013297	28 kDa heat- and acid-stable phosphoprotein	0.572	0.0112
IPI00012837	Kinesin heavy chain	0.587	0.0323
IPI00220301	Peroxiredoxin-6	0.636	0.0056
IPI00479997	Stathmin	0.652	0.0182
IPI00413108	Ribosomal protein SA	0.653	0.0134
IPI00001639	Importin β-1subunit	0.666	0.0002
IPI00387144	Tubulin α-ubiquitous chain	0.672	0.0003
IPI00418471	Vimentin	0.678	0.0077
IPI00554737	Serine/threonine-protein phosphatase 2A 65 kDa regulatory subunit A	0.681	0.0487
IPI00007752	Tubulin β-2C chain	0.683	0.0199
IPI00011654	Tubulin β chain	0.694	0.0317
IPI00023048	Elongation factor 1-delta	0.701	0.0036
IPI00000643	BAG family molecular chaperone regulator 2	0.727	0.0266
IPI00396485	Elongation factor 1-α 1	0.729	0.0353
IPI00419473	Isoform 2 of Transcription factor BTF3	0.736	0.0271
IPI00216587	40S ribosomal protein S8	0.739	0.0485
IPI00014537	Isoform 1 of Calumenin precursor	0.741	0.0297
IPI00645078	Ubiquitin-activating enzyme E1	0.749	0.0162
IPI00008433	40S ribosomal protein S5	0.763	0.0260
IPI00027230	Endoplasmin precursor	0.767	0.0344
IPI00306332	60S ribosomal protein L24	0.774	0.0348
IPI00221092	40S ribosomal protein S16	0.776	0.0284
IPI00023785	Isoform 1 of Probable ATP-dependent RNA helicase DDX17	0.777	0.0425
IPI00216975	TPM4 Isoform 2 of Tropomyosin α-4 chain	0.778	0.0358
IPI00013296	40S ribosomal protein S18	0.779	0.0143
IPI00014263	Isoform Long of Eukaryotic translation initiation factor 4H	0.789	0.0125
IPI00328748	ARMET protein precursor	0.791	0.0411
IPI00009235	Translocon-associated protein subunit γ	0.792	0.0403
IPI00156689	Synaptic vesicle membrane protein VAT-1 homolog	0.796	0.0229
IPI00045396	Isoform 2 of Calumenin precursor	0.798	0.0126
IPI00009904	Protein disulfide-isomerase A4 precursor	0.806	0.0489
IPI00332936	Isoform 2 of Zinc finger CCCH type antiviral protein 1	0.811	0.0142
IPI00000877	150 kDa oxygen-regulated protein precursor	0.812	0.0166
IPI00216134	Tropomyosin 1 α chain isoform 7	0.819	0.0179
IPI00383581	Isoform 1 of Neutral α-glucosidase AB precursor	0.819	0.0058
IPI00010796	Protein disulfide-isomerase precursor	0.823	0.0156
IPI00220709	Isoform 2 of Tropomyosin β chain	0.824	0.0259
IPI00063234	PRKAR2A protein	0.834	0.0246
IPI00646304	Peptidylprolyl isomerase B precursor	0.874	0.0429
IPI00027497	Glucose-6-phosphate isomerase	0.884	0.0315
IPI00215893	Heme oxygenase 1	0.904	0.0197
IPI00020599	Calreticulin precursor	0.918	0.0186
Depleted proteins			
IPI00027397	Isoform 1 of Hematological and neurological expressed 1-like protein	1.062	0.0471
IPI00031697	Transmembrane protein 109 precursor	1.102	0.0253
IPI00028946	Isoform 3 of Reticulon-3	1.148	0.0131
IPI00297910	Tumor-associated calcium signal transducer 2 precursor	1.172	0.0002
IPI00385449	Protein kinase C α type	1.192	0.0086
IPI00021076	Isoform Long of Plakophilin-4	1.226	0.0018

Table 1. Continued

ProteinID	Protein	Mean ratio[a)]	*p*-Value
IPI00075248	Calmodulin	1.251	0.0261
IPI00029730	Syntaxin-4	1.252	0.0409
IPI00023605	Isoform 1 of Cdc42 effector protein 1	1.261	0.0232
IPI00414005	Isoform short of sodium/potassium-transporting ATPase α-1 chain	1.275	0.0398
IPI00017292	Isoform 1 of Catenin β-1	1.279	0.0396
IPI00007755	Ras-related protein Rab-21	1.297	0.0304
IPI00293427	E3 ubiquitin-protein ligase ZNRF2	1.299	0.0397
IPI00418169	Annexin A2 isoform 1	1.312	0.0366
IPI00398435	Similar to Plexin-B2 precursor	1.313	0.0493
IPI00012512	Ras-related protein R-Ras2 precursor	1.315	0.0484
IPI00217563	Isoform β-1A of Integrin β-1 precursor	1.317	0.0285
IPI00215995	Isoform α-3A of Integrin α-3 precursor	1.326	0.0061
IPI00220194	Solute carrier family 2. facilitated glucose transporter member 1	1.328	0.0162
IPI00215948	Isoform 1 of Catenin α-1	1.331	0.0386
IPI00010438	Isoform SNAP-23a of Synaptosomal-associated protein 23	1.346	0.0076
IPI00020557	Low-density lipoprotein receptor-related protein 1 precursor	1.348	0.0255
IPI00216546	Isoform 2 of Probable palmitoyltransferase ZDHHC5	1.354	0.0009
IPI00302592	Filamin A α	1.365	0.0429
IPI00742780	FLJ00279 protein (Fragment)	1.369	0.0432
IPI00183002	Isoform 1 of protein phosphatase 1 regulatory subunit 12A	1.389	0.0185
IPI00645194	Integrin β 1	1.402	0.0460
IPI00414320	Annexin A11	1.409	0.0071
IPI00019997	Lin-7 homolog C	1.409	0.0162
IPI00011578	Isoform 1 of Neuroplastin precursor	1.413	0.0337
IPI00550234	Isoform 1 of Actin-related protein 2/3 complex subunit 5	1.416	0.0390
IPI00033494	Myosin regulatory light chain	1.436	0.0161
IPI00007058	Coronin-1B	1.459	0.0203
IPI00027422	Isoform β-4C of Integrin β-4 precursor	1.467	0.0072
IPI00006034	Cysteine-rich protein 2	1.489	0.0053
IPI00790010	Engulfment adaptor PTB domain containing 1	1.503	0.0167
IPI00021440	Actin cytoplasmic 2	1.519	0.0138
IPI00220991	Isoform 2 of AP-2 complex subunit β	1.542	0.0244
IPI00028911	Dystroglycan precursor	1.542	0.0241
IPI00337415	Guanine nucleotide-binding protein G(i). α-1 subunit	1.551	0.0092
IPI00335168	Isoform Non-muscle of Myosin light polypeptide 6	1.556	0.0332
IPI00554521	Ferritin heavy chain	1.567	0.0331
IPI00003348	Guanine nucleotide-binding protein G(I)/G(S)/G(T) subunit β 2	1.581	0.0355
IPI00438286	Isoform 1 of Protein LAP2	1.603	0.0498
IPI00550363	Transgelin-2	1.607	0.0375
IPI00219682	Stomatin	1.616	0.0016
IPI00216682	Calponin-3	1.634	0.0157
IPI00217059	Isoform 2 of Coiled-coil domain-containing protein 50	1.663	0.0142
IPI00020228	Frizzled-6 precursor	1.690	0.0420
IPI00220578	Guanine nucleotide-binding protein G	1.762	0.0029
IPI00015973	Band 4.1-like protein 2	1.869	0.0236
IPI00464981	Isoform 1 of Protein ITFG3	1.899	0.0442
IPI00397949	G protein-coupled receptor 56 isoform b	2.194	0.0282
IPI00465071	TBC domain containing protein 10B	2.268	0.0060
IPI00018219	Transforming growth factor-β-induced protein ig-h3 precursor	2.692	0.0001

a) The mean ratio is the average ratio from three independent SILAC experiments.

proteins predicted to be of ER or ribosomal origin were mainly enriched in the Golgi-enriched fraction upon infection with *Salmonella*, whereas those annotated to originate from the plasma membrane, mitochondrion and endosomes were mainly depleted.

The identified proteins were also categorized according to their molecular function annotation (Fig. 3A). The distribution of the majority of molecular function groups did not differ much between the identified and the affected proteins. It appeared that among the affected proteins, those with a CYT, select calcium-binding (SCB) or isomerase (ISO) classification were overrepresented. Next, we again differentiated between the enriched and depleted proteins in the isolated fraction upon infection, and determined their

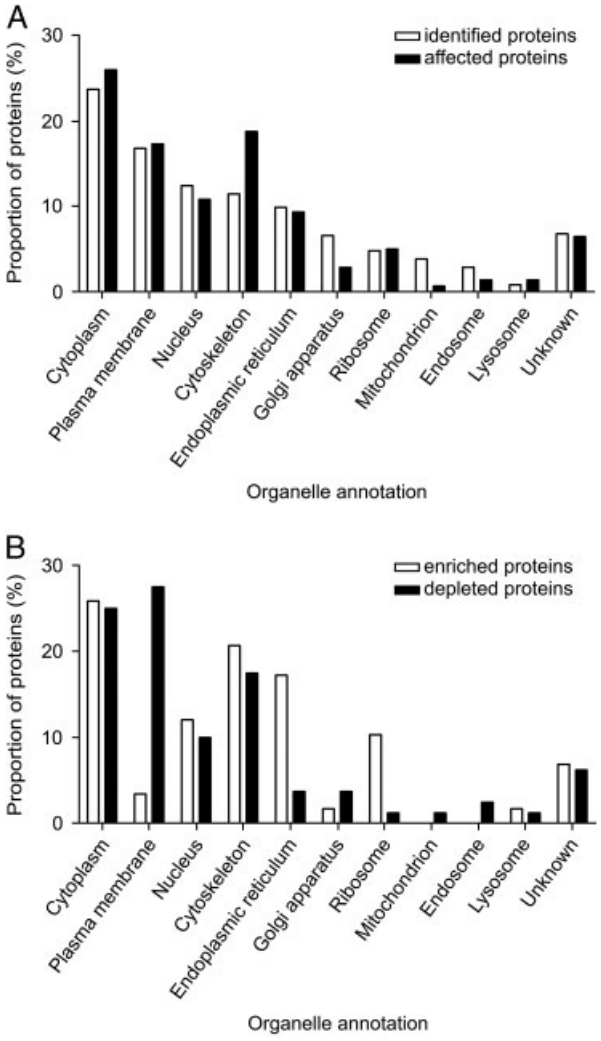

Figure 2. Subcellular localization of identified proteins. The subcellular localizations of the proteins were based on the annotations of UniProt. The distribution of the affected proteins was compared with that of all the identified proteins (A). The affected proteins were also categorized for the enriched and depleted proteins separately (B). Some proteins have more than one annotation, therefore the sum of each category can be higher than 100%.

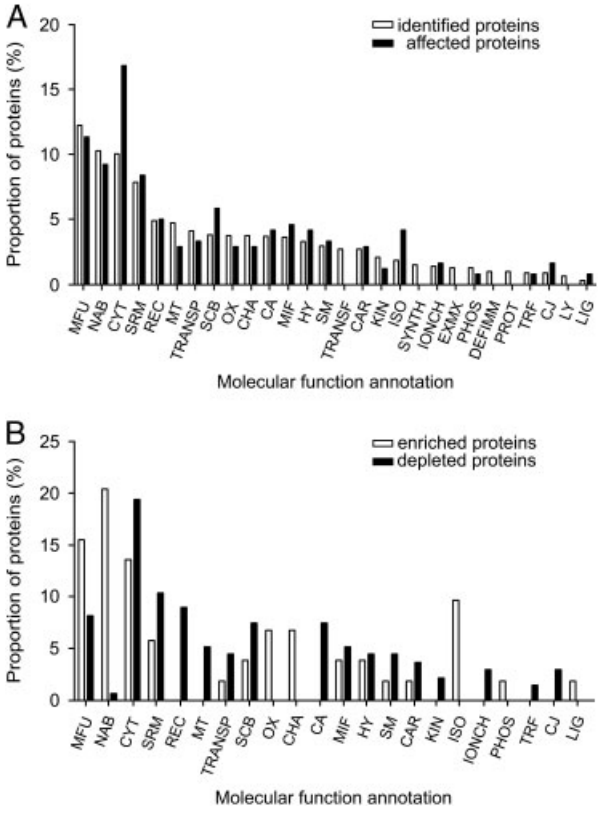

Figure 3. Molecular functions of identified proteins. The molecular functions of the proteins were based on the annotations of the PANTHER classification system. The distribution of the affected proteins was compared with that of all the identified proteins (A). The affected proteins were also categorized for the enriched and depleted proteins separately (B). Some proteins have more than one annotation, therefore the sum of each category can be higher than 100%. MFU, molecular function unclassified; NAB, nucleic acid binding protein; CYT, cytoskeletal protein; SRM, select regulatory molecule; REC, receptor; MT, membrane traffic protein; TRANSP, transporter; SCB, select calcium-binding protein; OX, oxireductase; CHA, chaperone; CA, cell adhesion molecule; MIF, miscellaneous function; HY, hydrolase; SM, signaling molecule; TRANSF, transferase; CAR, transfer/carrier protein; KIN, kinase; ISO, isomerase; SYNTH, synthase and synthetase; IONCH, ion channel protein; EXMX, extracellular matrix protein; PHOS, phosphatase; DEFIMM, defense/immunity protein; PROT, protease; TRF, transcription factor; CJ, cell junction protein; LY, lyase; LIG, ligase.

distribution according to their molecular function (Fig. 3B). The CYT and SCB groups contained both enriched and depleted proteins, whereas the membrane traffic proteins (MT) were all depleted in the Golgi-enriched fraction upon infection.

3.3 Functional relevance of selected protein hits

By performing RNA interference experiments, we validated the functional relevance of affected proteins in the *Salmonella* infection cycle. From the 105 affected proteins, 21 proteins were selected (Table 2). The 21 selected proteins covered 9 different molecular function groups and were predicted to localize to 6 different organelles. Both enriched and depleted proteins were selected. HeLa cells were depleted for each of the 21 selected proteins by transfecting cells with siRNA oligos targeting each selected protein. Forty-eight hours post-transfection the cells were infected with wt *S. typhimurium* for 8 h. The mean fold increase in *Salmonella* replication was calculated for each condition as described in Section 2.

Figure 4A depicts the differences in *Salmonella* replication in HeLa cells depleted for the selected proteins, as

Table 2. 21 selected candidates for the siRNA experiments

Selected candidate	Gene symbol	Mean ratio[a)]	MF annotation[b)]	Organelle annotation[c)]
Enriched proteins				
Stanniocalcin-2 precursor	STC2	0.22	M	
Solute carrier family 38 member 2	SLC38A2	0.22	MFU	PM
A-kinase anchor protein 12 isoform 2	AKAP12	0.55	MFU	CP/CYT
28 kDa heat- and acid-stable phosphoprotein	PDAP1	0.57	MFU	?
Kinesin heavy chain	KIF5B	0.59	CYT	CP/CYT
Peroxiredoxin-6	PRDX6	0.64	OX	CP/L
Depleted proteins				
Coronin-1B	CORO1B	1.46	CYT	CP/CYT
Isoform β-4C of Integrin β-4 precursor	ITGB4	1.47	MFU	PM
Engulfment adaptor PTB domain containing 1	GULP1	1.50	SM	CP
Isoform 2 of AP-2 complex subunit β	AP2B1	1.54	MT	CP/PM
Guanine nucleotide-binding protein G(i), α-1 subunit	GNAI1	1.55	SRM	PM
Ferritin heavy chain	FTH1	1.57	MIF	CP
Guanine nucleotide-binding protein G(I)/G(S)/G(T) subunit b2	GNB2	1.58	SRM/HY	CP
Isoform 1 of Protein LAP2	ERBB2IP	1.60	MIF	N/CP/PM
Stomatin	STOM	1.62	CYT	CYT/PM
Frizzled-6 precursor	FZD6	1.69	MFU	PM
Guanine nucleotide-binding protein G	GNAI3	1.76	SRM	G/CP/PM
Band 4,1-like protein 2	EPB41L2	1.87	MFU	CYT/PM
Isoform 1 of Protein ITFG3	ITFG3	1.90	MFU	?
G protein-coupled receptor 56 isoform b	GPR56	2.19	REC	PM
TBC domain containing protein 10B	TBC1D10B	2.27	SRM	?

a) The mean ratio is the average ratio from three independent SILAC experiments.
b) Molecular Function annotation: SM, signaling molecule; MFU, molecular function unclassified; CYT, cytoskeletal protein; OX, oxireductase; MT, membrane traffic; SRM, select regulatory molecule; MIF, miscellaneous function; HY, hydrolase; REC, receptor.
c) ?, unknown; PM, plasma membrane; CP, cytoplasm; CYT, cytoskeleton; L, lysosome; N, nucleus; G, Golgi apparatus.

compared with HeLa cells transfected with control (scrambled) siRNA. Interestingly, depletion of peroxiredoxin-6 (PRDX6), isoform β-4c of integrin β-4 (ITGB4), isoform 1 of protein lap2 (erbin interacting protein; ERBB2IP), stomatin (STOM) or TBC domain containing protein 10b (TBC1D10B) led to a >two-fold increased *Salmonella* replication. Depletion of most other proteins did not lead to a major change in *Salmonella* replication.

As a control for the siRNA transfection efficiency, mRNA degradation of PRDX6, ITGB4, ERBB2IP, STOM and TBC1D10B was assessed by quantitative RT-PCR. As shown in Fig. 4B, transfection of the different siRNA oligos led to a significant reduction (>85–95%) in the amount of mRNA encoding each of the five proteins when compared to cells transfected with control siRNA oligos.

3.4 Protein patterns in uninfected and *Salmonella*-infected cells

We determined the potential subcellular relocation of PRDX6, ITGB4, ERBB2IP, STOM or TBC1D10B upon infection. Using appropriate antibodies we were, however, unsuccessful at the immunofluorescence (IF) level to show significant changes in subcellular localization upon infection. This does, however, not exclude relocation of affected proteins as relocation of small (catalytic) amounts of protein to/from another organelle may have a strong effect at e.g. the Golgi complex. Since no evidence for appreciable relocation of affected proteins could be gleaned from IF microscopy, we also investigated alterations in expression levels as a mean to significantly change the amount of protein in the Golgi-enriched fraction. To this end we compared the protein levels of STOM, TBC1D10B and PRDX6 in PNS of uninfected versus infected cells using Western blot analysis. As shown in Fig. 5, the cellular protein expression level of STOM, TBC1D10B and PRDX6 (and also of the controls, GαGβ and β-actin) did not change upon infection.

3.5 STOM and ITGB4 depletion leads to a dispersal of *Salmonella* microcolonies

To investigate whether the depletion of PRDX6, ITGB4, ERBB2IP, STOM or TBC1D10B also had an effect on the *Salmonella* microcolony morphology, cells were transfected with the siRNA oligos and infected with *Salmonella* (as described above), after which the microcolonies were analyzed by confocal microscopy. Two different phenotypes were observed: tight and dispersed microcolonies. Representative images used for the confocal analysis are shown in

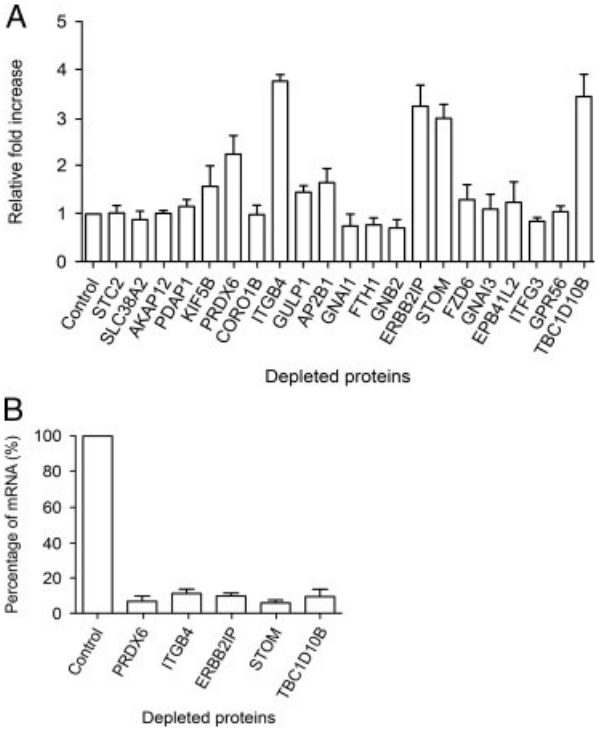

Figure 4. Functional relevance of the selected proteins. HeLa cells were transfected with siRNA oligos targeting the selected proteins for 48 h and infected with wt *Salmonella* for 8 h. The differences in *Salmonella* replication in the interfered cells are depicted as the mean fold increase expressed relative to cells treated with control siRNAs (A). The efficiency of mRNA degradation after transfection of siRNA oligos targeting PRDX6, ITGB4, ERBB2IP, STOM and TBC1D10B is shown in (B). The results of three independent experiments are shown. Error bars indicate standard deviations.

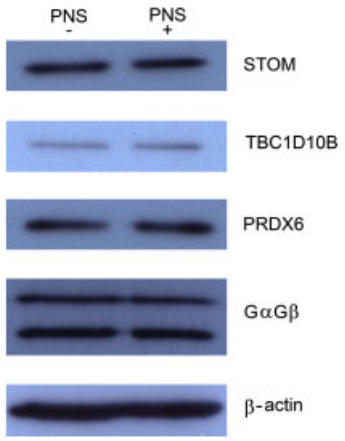

Figure 5. Western blot analysis of protein pattern in uninfected and infected cells. PNS obtained from mock-infected (PNS-) and *Salmonella*-infected (PNS+) cells were loaded (30 μg protein for each PNS sample) and stained for three of the affected proteins (STOM, TBC1D10B and PRDX6) as well as two controls (GαGβ and β-actin).

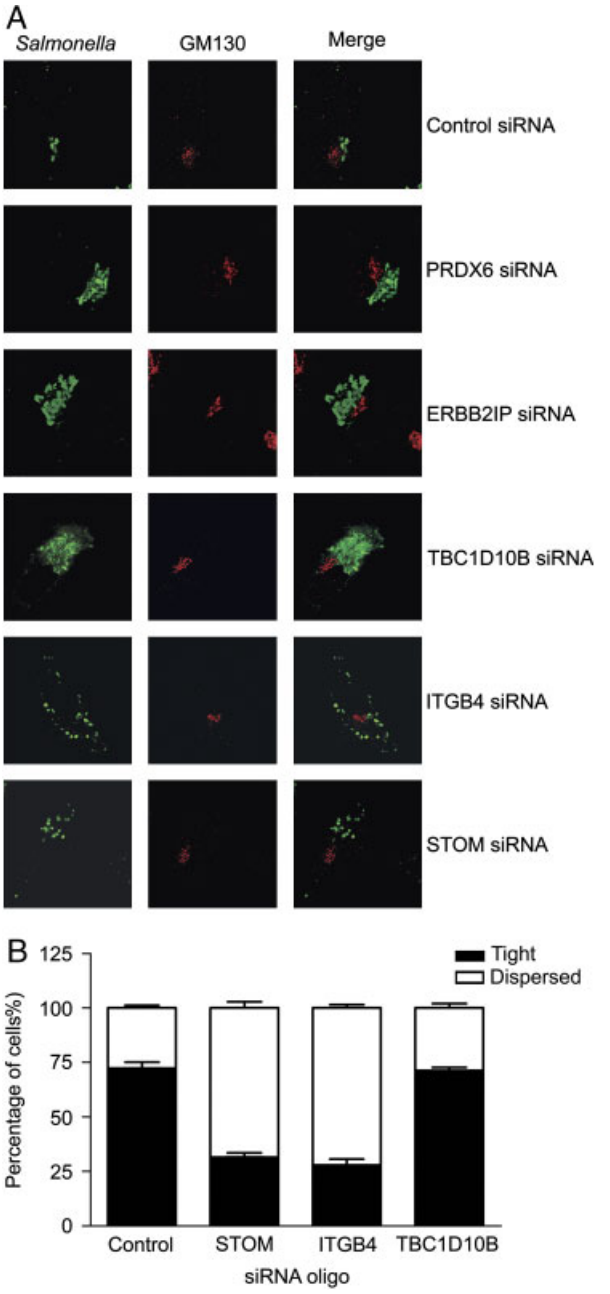

Figure 6. Changed morphology of *Salmonella* microcolonies upon depletion of STOM or ITGB4. HeLa cells were transfected with siRNA oligos targeting PRDX6, ITGB4, ERBB2IP, STOM or TBC1D10B and infected with wt *Salmonella* for 6 h. Cells were stained with anti-LPS and anti-GM130 antibodies. The morphology of *Salmonella* microcolonies in cells depleted of the five proteins is shown in (A). In green is the anti-LPS staining, identifying the *Salmonella* microcolony, and in red is the anti-GM130 (Golgi) staining. Quantification of the degree of dispersal of the microcolonies due to depletion of STOM, ITGB4 or TBC1D10B is shown in (B). Three independent experiments were performed in which 100 HeLa cells per condition were analyzed.

Fig. 6A. The control cells mainly contained tight *Salmonella* microcolonies in the Golgi region. Strikingly, however, depletion of STOM or ITGB4 resulted in a dispersal of *Salmonella* bacteria throughout the cytoplasm. Depletion of TBC1D10B, ERBB2IP or PRDX6 did not show this dispersal effect. The phenotype of the microcolonies after depletion of STOM or ITGB4 was also quantified by counting the microcolonies of 100 HeLa cells per condition in three independent experiments (Fig. 6B). Approximately, 75% of the control cells contained tight microcolonies, whereas the majority of STOM- or ITGB4-depleted HeLa cells contained dispersed microcolonies. As an additional control, the microcolony phenotype in TBC1D10B-depleted HeLa cells was also quantified. Similar to the control cells, approximately 75% of the TBC1D10B-depleted cells contained tight microcolonies.

4 Discussion

During invasion and replication in cells, *Salmonella* delivers more than 30 effectors into the host cell cytosol to control SCV maturation by modulating its interaction with diverse intracellular compartments. Many of the host proteins that are involved in these interactions remain to be identified. Detailed insight into *Salmonella*–host interactions is important for our understanding of *Salmonella* infection and may also lead to new possibilities for therapeutic intervention. In a previous report [33] we applied SILAC-based quantitative proteomics to investigate coronavirus–host interactions. In this study, we used the same approach to study *Salmonella* infection in epithelial cells. Because of the known role of the secretory pathway, and more specifically the Golgi apparatus, in the infection cycle of *Salmonella,* we focused our attention on isolated Golgi-enriched fractions. We compared protein abundances in these fractions isolated from *Salmonella*- and mock-infected HeLa cells. We identified 105 proteins that changed in abundance in the Golgi-enriched fractions upon *Salmonella* infection. The functional relevance of a subset of these proteins was examined using siRNA-mediated depletion and for five proteins this was shown to lead to an increased *Salmonella* replication.

To obtain more insight into the proteins that changed significantly in abundance upon *Salmonella* infection, the identified proteins were grouped according to their organellar and molecular function annotation. Proteins annotated to be localized to several cellular compartments were found in the Golgi-enriched fraction. This is not unexpected as our Golgi isolation procedure is based on established protocols that show a maximal 52-fold enrichment of Golgi markers, with a 1–4-fold enrichment of protein markers from other organelles [35–37]. Of note, proteins localizing primarily in other organelles than the Golgi may very well also be present in the Golgi, albeit at lower levels. We identified 765 proteins in the Golgi-enriched fraction from which 105 were affected upon *Salmonella* infection. From Figs. 2 and 3 it is clear that *Salmonella* infection affected proteins from several different groups. Proteins predicted to associate with the cytoskeleton/annotated to the CYT function group (Figs. 2 and 3) were consistently affected. This is in agreement with several reports showing that *Salmonella* infection affects the cytoskeleton during entry and movement to the Golgi region in order to establish a replicating niche [17, 28, 46–48]. Some of the affected CYT proteins in the Golgi-enriched fraction were increased in abundance, whereas others were decreased. It remains to be established whether a change in the location of a cytoskeleton-associated protein is initiated either by *Salmonella* to promote its replication, or by the host cell to elicit an immune response. In addition, proteins annotated to the membrane traffic group, mainly predicted to localize to the Golgi apparatus/endosomes, were consistently affected upon *Salmonella* infection. The majority of those proteins were depleted from the Golgi fraction upon *Salmonella* infection. The depletion of these affected proteins from the Golgi region upon *Salmonella* infection might be the result of relocation of these proteins away from the Golgi either induced by the bacterium for its own benefit or by the host cell as a defense mechanism. Our preliminary data (RT-PCR analysis of mRNA levels in uninfected vs infected cells) indicated that the affected proteins are not down regulated, suggesting that the change in their abundance in the Golgi more likely results from altered membrane dynamics/protein relocation than from altered protein degradation/altered gene expression (data not shown). These data were confirmed by comparison of protein levels (STOM, TBC1D10B and PRDX6) in PNS of uninfected versus infected cells using Western blot analysis (Fig. 5). The results showed that at least for STOM, TBC1D10B and PRDX6 the cellular protein expression level did not change upon infection and suggest that relocation of these proteins is a likely cause of depletion or enrichment in the Golgi-enrieched fraction. As a (loading) control for this experiment, antibodies recognizing GαGβ and β-actin were used. As can be seen in Fig. 5, the signal for these proteins is the same in uninfected and infected PNS.

Of note, because of the (SILAC) procedure it is highly unlikely that the affected abundance of the CYT proteins and/or membrane traffic proteins that we observed during *Salmonella* infection is the result of cellular contamination. If an indentified protein (Table 1) would be present as a result of impurities, this protein will be present in isolated fractions from infected as well as from uninfected cells, resulting in a ratio of 1 (Fig. 1). In addition, when we use the same (SILAC) approach to investigate coronavirus infections [33], there is no overlap in identified proteins, illustrating the specificity of the identified proteins for *Salmonella* infections.

To study the functional relevance of the affected proteins in *Salmonella* replication, siRNA experiments were performed for a selected subset of these proteins. Depletion of PRDX6, ITGB4, ERBB2IP, STOM or TBC1D10B resulted

in a >two-fold increase of *Salmonella* replication. In addition to the effect of these five proteins on *Salmonella* replication, depletion of STOM or ITGB4 resulted in a dispersal of the *Salmonella* microcolony (Fig. 6). This is an interesting phenotype, although with our present knowledge, hard to explain. Efficient *Salmonella* replication in epithelial cells is known to be dependent on tight microcolonies that are surrounded by intact Golgi membranes. Dispersed microcolonies were shown to result in decreased replication by others before [29]. However, in our case, cells that are depleted of STOM or ITGB4, show an increased *Salmonella* replication, despite of (or because of) dispersed microcolonies. This interesting phenotype is currently subject of further investigation.

In our assay system, PRDX6 was enriched in the isolated Golgi-enriched fraction from *Salmonella*-infected cells, while ITGB4, ERBB2IP, STOM and TBC1D10B were depleted in these fractions. Despite the difference in the effect of infection on the abundance in the Golgi fraction of PRDX6 on the one hand, and that of the other four proteins on the other hand, depletion of each of the five proteins by siRNA led to increased *Salmonella* replication. Although at first sight this may look like a discrepancy, it should be kept in mind that the siRNA treatment leads to depletion of the respective proteins in the whole cell, whereas the changes in abundance upon infection in our assay system were observed in isolated Golgi fractions. Moreover, with our current knowledge we cannot say whether the effects on the abundance of the five proteins seen in the Golgi fraction reflect changes initiated by the *Salmonella* to promote its own replication or changes initiated by the host cell to inhibit *Salmonella* replication. This may, of course, differ for the various proteins.

Below we will briefly discuss the five proteins that affected *Salmonella* replication.

PRDX6 is a member of the peroxiredoxin family of antioxidant enzymes. It is a bifunctional enzyme that has both glutathione peroxidase and phospholipase A_2 (PLA_2) enzymatic activities [49]. As the PLA_2 activity of PRX6 is maximal at acidic pH, it was suggested that PRDX6 has a lysosomal localization [50–52]. Recently, another report has shown that PRDX6 can be translocated to the plasma membrane where its PLA_2 activity can be activated [53]. A function of PRDX6 in *Salmonella* infection has not been described, but as the SCV has several interactions with the endo/lysosomal pathway during maturation, PRDX6 might as well be involved in those interactions. Furthermore, PRDX6 might also interfere with the oxidative stress response that is induced by the host cell upon *Salmonella* infection.

ITGB4 is a member of the integrin family, which are transmembrane glycoprotein receptors that mediate cell–matrix and cell–cell adhesion. They also transduce signals that regulate gene expression and cell growth. Integrins are composed of different combinations of α and β subunits that differ in their ligand binding specificity. The role of ITGB4 in *Salmonella* infection has not been elucidated so far. Interestingly, ITGB4 has been shown to bind to ERBB2IP (a.k.a. ERBIN and LAP2 [54]) that was also found in our screen. Members of the LAP (leucine-rich repeats and PDZ domains) family of proteins are involved in maintaining the shape and apical-basal polarity of epithelial cells [55]. ERBB2IP has been found to bind to Nod2 in epithelial cells infected with *Shigella flexneri* [56]. Nod2 is a member of the NACHT-LRR proteins (NLRs) that can sense bacterial components in order to elicit an immune response [57]. It is localized to the cell membrane and this localization is important for its bacterium-sensing function [58]. Kufer et al. [56] showed that ERBB2IP and Nod2 partially co-localize at the cell membrane and at the entry foci during infection with *Shigella*. It was furthermore shown that ERBB2IP acts as a negative regulator of Nod2 signaling [59]. The decreased amount of ERBB2IP in the Golgi fraction isolated from HeLa cells infected by *Salmonella* may reflect a relocation of ERBB2IP, resulting in changed dynamics of the Nod2/ERBB2IP complex. This was also shown in *Shigella* infection [52] although the biological relevance of this observation remains to be established.

TBC1D10B is a member of the Tre-2/Bub2/Cdc16 (TBC) domain-containing proteins. The TBC domain is a conserved protein motif that functions as a Rab GTPase-activating protein (Rab-GAP). TBC1D10B was shown to function as a Rab-GAP for Rab3A, Rab22A, Rab27A and Rab35 [60]. Smith et al. [61] studied the association of various Rabs with SCVs that either contain wt *Salmonella* or a non-invasive *Salmonella* mutant that travels to late endocytic compartments (considered the model phagosome). Eighteen Rabs were found to be associated with the maturing SCV. Rab35 was not present on wt SCVs but was associated with the model phagosomes, which suggests a role for Rab35 in phagosome maturation [61]. Since TBC1D10B was depleted from our Golgi fraction upon *Salmonella* infection, this may suggest an affected Rab35 activation and thereby an affected SCV maturation.

STOM is a multifunctional integral membrane protein. It associates with lipid rafts [62] and is suggested to regulate ion channel function or to act as a CYT anchor [63–67]. Furthermore, STOM has been shown to associate with lipid droplets that interact with other vesicles in the cell [68]. Lipid droplets accumulate in the surroundings of the SCV. This interaction may be involved in the supply of elevated levels of cholesterol on the SCV that become esterified by a *Salmonella* effector [69]. Whether STOM plays a role in this process remains to be established.

In summary, we have identified 105 proteins that were significantly affected during *Salmonella* infection. Depletion of only a small subset of these proteins already identified five host factors involved in *Salmonella* replication. PRDX6, ITGB4, ERBB2IP, STOM and TBC1D10B all have different functions, which can shed new light on the details of *Salmonella*–host interactions. Therefore, these five proteins will be subjects of further

investigations aimed at elucidating the interplay between *Salmonella* and epithelial cells.

This work was financially supported by the Faculty of Veterinary Medicine of Utrecht University, The Netherlands. The authors thank Ruud Eerland for assistance with the Salmonella replication assays and Richard Wubbolts (centre for cellular imaging (CCI) from the faculty of Veterinary Medicine, Utrecht University) for assistance with analyzing the confocal images. The authors acknowledge the Netherlands Proteomics Centre, embedded in the Netherlands Genomics Initiative, for support and access to the mass spectrometry facilities.

The authors have declared no conflict of interest.

5 References

[1] Ohl, M. E., Miller, S. I., *Salmonella*: a model for bacterial pathogenesis. *Annu. Rev. Med.* 2001, *52*, 259–274.

[2] Tsolis, R. M., Kingsley, R. A., Townsend, S. M., Ficht, T. A. et al., Of mice, calves, and men. Comparison of the mouse typhoid model with other *Salmonella* infections. *Adv. Exp. Med. Biol.* 1999, *473*, 261–274.

[3] Santos, R. L., Zhang, S., Tsolis, R. M., Kingsley, R. A. et al., Animal models of *Salmonella* infections: enteritis versus typhoid fever. *Microbes Infect.* 2001, *3*, 1335–1344.

[4] Jones, B. D., Ghori, N., Falkow, S., *Salmonella typhimurium* initiates murine infection by penetrating and destroying the specialized epithelial M cells of the Peyer's patches. *J. Exp. Med.* 1994, *180*, 15–23.

[5] Santos, R. L., Bäumler, A. J., Cell tropism of *Salmonella enterica*. *Int. J. Med. Microbiol.* 2004, *294*, 225–233.

[6] Rescigno, M., Urbano, M., Valzasina, B., Francolini, M. et al., Dendritic cells express tight junction proteins and penetrate gut epithelial monolayers to sample bacteria. *Nat. Immunol.* 2001, *2*, 361–367.

[7] Hueck, C. J., Type III protein secretion systems in bacterial pathogens of animals and plants. *Microbiol. Mol. Biol. Rev.* 1998, *62*, 379–433.

[8] Cornelis, G. R., Van Gijsegem, F., Assembly and function of type III secretory systems. *Annu. Rev. Microbiol.* 2000, *54*, 735–774.

[9] Schraidt, O., Lefebre, M. D., Brunner, M. J., Schmied, W. H. et al., Topology and organization of the *Salmonella typhimurium* type III secretion needle complex components. *PLoS Pathog.* 2010, *6*, e1000824.

[10] Galán, J. E., Wolf-Watz, H., Protein delivery into eukaryotic cells by type III secretion machines. *Nature* 2006, *444*, 567–573.

[11] He, S. Y., Nomura, K., Whittam, T. S., Type III protein secretion mechanism in mammalian and plant pathogens. *Biochim. Biophys. Acta* 2004, *1694*, 181–206.

[12] Galán, J. E., *Salmonella* interactions with host cells: type III secretion at work. *Annu. Rev. Cell Dev. Biol.* 2001, *17*, 53–86.

[13] Hansen-Wester, I., Hensel, M., *Salmonella* pathogenicity islands encoding type III secretion systems. *Microbes Infect.* 2001, *3*, 549–559.

[14] Hensel, M., *Salmonella* pathogenicity island 2. *Mol. Microbiol.* 2000, *36*, 1015–1023.

[15] Steele-Mortimer, O., Brumell, J. H., Knodler, L. A., Méresse, S. et al., The invasion-associated type III secretion system of *Salmonella enterica* serovar Typhimurium is necessary for intracellular proliferation and vacuole biogenesis in epithelial cells. *Cell Microbiol.* 2002, *4*, 43–54.

[16] Waterman, S. R., Holden, D. W., Functions and effectors of the *Salmonella* pathogenicity island 2 type III secretion system. *Cell Microbiol.* 2003, *5*, 501–511.

[17] Finlay, B. B., Ruschkowski, S., Dedhar, S., Cytoskeletal rearrangements accompanying *Salmonella* entry into epithelial cells. *J. Cell Sci.* 1991, *99*, 283–296.

[18] Francis, C. L., Ryan, T. A., Jones, B. D., Smith, S. J., Falkow, S., Ruffles induced by *Salmonella* and other stimuli direct macropinocytosis of bacteria. *Nature* 1993, *364*, 639–642.

[19] Chen, L. M., Hobbie, S., Galán, J. E., Requirement of CDC42 for *Salmonella*-induced cytoskeletal and nuclear responses. *Science* 1996, *274*, 2115–2118.

[20] Hardt, W. D., Chen, L. M., Schuebel, K. E., Bustelo, X. R., Galan, J. E., *S. typhimurium* encodes an activator of Rho GTPases that induces membrane ruffling and nuclear responses in host cells. *Cell* 1998, *93*, 815–826.

[21] Bakowski, M. A., Braun, V., Brumell, J. H., *Salmonella*-containing vacuoles: directing traffic and nesting to grow. *Traffic* 2008, *9*, 2022–2031.

[22] Gorvel, J. P., Méresse, S., Maturation steps of the *Salmonella*-containing vacuole. *Microbes Infect* 2001, *3*, 1299–1303.

[23] Knodler, L. A., Steele-Mortimer, O., Taking possession: biogenesis of the *Salmonella*-containing vacuole. *Traffic* 2003, *4*, 587–599.

[24] Ramsden, A. E., Holden, D. W., Mota, L. J., Membrane dynamics and spatial distribution of *Salmonella*-containing vacuoles. *Trends Microbiol.* 2007, *15*, 516–524.

[25] Steele-Mortimer, O., The *Salmonella*-containing vacuole: moving with the times. *Curr. Opin. Microbiol.* 2008, *11*, 38–45.

[26] Steele-Mortimer, O., Méresse, S., Gorvel, J. P., Toh, B. H., Finlay, B. B., Biogenesis of *Salmonella typhimurium*-containing vacuoles in epithelial cells involves interactions with the early endocytic pathway. *Cell Microbiol.* 1999, *1*, 33–49.

[27] Abrahams, G. L., Müller, P., Hensel, M., Functional dissection of SseF, a type III effector protein involved in positioning the *Salmonella*-containing vacuole. *Traffic* 2006, *7*, 950–965.

[28] Deiwick, J., Salcedo, S. P., Boucrot, E., Gilliland, S. M. et al., The translocated *Salmonella* effector proteins SseF and SseG interact and are required to establish an intracellular replication niche. *Infect. Immun.* 2006, *74*, 6965–6972.

[29] Salcedo, S. P., Holden, D. W., SseG, a virulence protein that targets *Salmonella* to the Golgi network. *Embo J.* 2003, *22*, 5003–5014.

[30] Ramsden, A. E., Mota, L. J., Munter, S., Shorte, S. L., Holden, D. W., The SPI-2 type III secretion system restricts motility of *Salmonella*-containing vacuoles. *Cell Microbiol.* 2007, *9*, 2517–2529.

[31] Kuhle, V., Abrahams, G. L., Hensel, M., Intracellular *Salmonella enterica* redirect exocytic transport processes in a *Salmonella* pathogenicity island 2-dependent manner. *Traffic* 2006, *7*, 716–730.

[32] Ong, S. E., Blagoev, B., Kratchmarova, I., Kristensen, D. B. et al., Stable isotope labeling by amino acids in cell culture, SILAC, as a simple and accurate approach to expression proteomics. *Mol. Cell. Proteomics* 2002, *1*, 376–386.

[33] Vogels, M. W., van Balkom, B. W., Kaloyanova, D. V., Batenburg, J. J. et al., Identification of host factors involved in coronavirus replication by quantitative proteomics analysis. *Proteomics* 2011, *11*, 64–80.

[34] Beuzón, C. R., Méresse, S., Unsworth, K. E., Ruiz-Albert, J. et al., *Salmonella* maintains the integrity of its intracellular vacuole through the action of SifA. *Embo J.* 2000, *19*, 3235–3249.

[35] Balch, W. E., Dunphy, W. G., Braell, W. A., Rothman, J. E., Reconstitution of the transport of protein between successive compartments of the Golgi measured by the coupled incorporation of *N*-acetylglucosamine. *Cell* 1984, *39*, 405–416.

[36] Brügger, B., Sandhoff, R., Wegehingel, S., Gorgas, K. et al., Evidence for segregation of sphingomyelin and cholesterol during formation of COPI-coated vesicles. *J. Cell Biol.* 2000, *151*, 507–518.

[37] Gkantiragas, I., Brügger, B., Stuven, E., Kaloyanova, D. et al., Sphingomyelin-enriched microdomains at the Golgi complex. *Mol. Biol. Cell* 2001, *12*, 1819–1833.

[38] Sohn, K., Orci, L., Ravazzola, M., Amherdt, M. et al., A major transmembrane protein of Golgi-derived COPI-coated vesicles involved in coatomer binding. *J. Cell Biol.* 1996, *135*, 1239–1248.

[39] van Balkom, B. W., van Gestel, R. A., Brouwers, J. F., Krijgsveld, J. et al., Mass spectrometric analysis of the *Schistosoma mansoni* tegumental sub-proteome. *J. Proteome Res.* 2005, *4*, 958–966.

[40] Kersey, P. J., Duarte, J., Williams, A., Karavidopoulou, Y. et al., The International Protein Index: an integrated database for proteomics experiments. *Proteomics* 2004, *4*, 1985–1988.

[41] Perkins, D. N., Pappin, D. J., Creasy, D. M., Cottrell, J. S., Probability-based protein identification by searching sequence databases using mass spectrometry data. *Electrophoresis* 1999, *20*, 3551–3567.

[42] Schulze, W. X., Mann, M., A novel proteomic screen for peptide-protein interactions. *J. Biol. Chem.* 2004, *279*, 10756–10764.

[43] van Breukelen, B., van den Toorn, H. W., Drugan, M. M., Heck, A. J., StatQuant: a post-quantification analysis toolbox for improving quantitative mass spectrometry. *Bioinformatics* 2009, *25*, 1472–1473.

[44] Steele-Mortimer, O., Infection of epithelial cells with *Salmonella enterica*. *Methods Mol. Biol.* 2008, *431*, 201–211.

[45] Thomas, P. D., Campbell, M. J., Kejariwal, A., Mi, H. et al., PANTHER: a library of protein families and subfamilies indexed by function. *Genome Res.* 2003, *13*, 2129–2141.

[46] Kuhle, V., Jackel, D., Hensel, M., Effector proteins encoded by *Salmonella* pathogenicity island 2 interfere with the microtubule cytoskeleton after translocation into host cells. *Traffic* 2004, *5*, 356–370.

[47] Méresse, S., Unsworth, K. E., Habermann, A., Griffiths, G. et al., Remodelling of the actin cytoskeleton is essential for replication of intravacuolar *Salmonella*. *Cell Microbiol.* 2001, *3*, 567–577.

[48] Miao, E. A., Brittnacher, M., Haraga, A., Jeng, R. L. et al., *Salmonella* effectors translocated across the vacuolar membrane interact with the actin cytoskeleton. *Mol. Microbiol.* 2003, *48*, 401–415.

[49] Manevich, Y., Fisher, A. B., Peroxiredoxin 6, a 1-Cys peroxiredoxin, functions in antioxidant defense and lung phospholipid metabolism. *Free Radic. Biol. Med.* 2005, *38*, 1422–1432.

[50] Fisher, A. B., Dodia, C., Yu, K., Manevich, Y., Feinstein, S. I., Lung phospholipid metabolism in transgenic mice overexpressing peroxiredoxin 6. *Biochim. Biophys. Acta* 2006, *1761*, 785–792.

[51] Kim, T. S., Dodia, C., Chen, X., Hennigan, B. B. et al., Cloning and expression of rat lung acidic Ca(2+)-independent PLA2 and its organ distribution. *Am. J. Physiol.* 1998, *274*, L750–L61.

[52] Kim, T. S., Sundaresh, C. S., Feinstein, S. I., Dodia, C. et al., Identification of a human cDNA clone for lysosomal type Ca^{2+}-independent phospholipase A2 and properties of the expressed protein. *J. Biol. Chem.* 1997, *272*, 2542–2550.

[53] Chatterjee, S., Feinstein, S. I., Dodia, C., Sorokina, E. et al., Peroxiredoxin 6 phosphorylation and subsequent phospholipase A2 activity are required for agonist-mediated activation of NADPH oxidase in mouse pulmonary microvascular endothelium and alveolar macrophages. *J. Biol. Chem.* 2011, *286*, 32427–32436.

[54] Favre, B., Fontao, L., Koster, J., Shafaatian, R. et al., The hemidesmosomal protein bullous pemphigoid antigen 1 and the integrin beta 4 subunit bind to ERBIN. Molecular cloning of multiple alternative splice variants of ERBIN and analysis of their tissue expression. *J. Biol. Chem.* 2001, *276*, 32427–32436.

[55] Bryant, P. J., Huwe, A., LAP proteins: what's up with epithelia? *Nat. Cell Biol.* 2000, *2*, E141–3.

[56] Kufer, T. A., Kremmer, E., Banks, D. J., Philpott, D. J., Role for erbin in bacterial activation of Nod2. *Infect. Immun.* 2006, *74*, 3115–3124.

[57] Girardin, S. E., Boneca, I. G., Viala, J., Chamaillard, M. et al., Nod2 is a general sensor of peptidoglycan through muramyl dipeptide (MDP) detection. *J. Biol. Chem.* 2003, *278*, 8869–8872.

[58] Barnich, N., Aguirre, J. E., Reinecker, H. C., Xavier, R., Podolsky, D. K., Membrane recruitment of NOD2 in intestinal epithelial cells is essential for nuclear factor-kappaB activation in muramyl dipeptide recognition. *J. Cell Biol.* 2005, *170*, 21–26.

[59] McDonald, C., Chen, F. F., Ollendorff, V., Ogura, Y. et al., A role for Erbin in the regulation of Nod2-dependent NF-kappaB signaling. *J. Biol. Chem.* 2005, *280*, 40301–40309.

[60] Ishibashi, K., Kanno, E., Itoh, T., Fukuda, M., Identification and characterization of a novel Tre-2/Bub2/Cdc16 (TBC) protein that possesses Rab3A-GAP activity. *Genes Cells* 2009, *14*, 41–52.

[61] Smith, A. C., Heo, W. D., Braun, V., Jiang, X. et al., A network of Rab GTPases controls phagosome maturation and is modulated by *Salmonella enterica* serovar Typhimurium. *J. Cell Biol.* 2007, *176*, 263–268.

[62] Snyers, L., Umlauf, E., Prohaska, R., Association of stomatin with lipid–protein complexes in the plasma membrane and the endocytic compartment. *Eur. J. Cell Biol.* 1999, *78*, 802–812.

[63] Hiebl-Dirschmied, C. M., Adolf, G. R., Prohaska, R., Isolation and partial characterization of the human erythrocyte band 7 integral membrane protein. *Biochim. Biophys. Acta* 1991, *1065*, 195–202.

[64] Wang, D., Mentzer, W. C., Cameron, T., Johnson, R. M., Purification of band 7.2b, a 31-kDa integral phosphoprotein absent in hereditary stomatocytosis. *J Biol Chem* 1991, *266*, 17826–17831.

[65] Stewart, G. W., Argent, A. C., Dash, B. C., Stomatin: A putative cation transport regulator in the red cell membrane. *Biochim. Biophys. Acta* 1993, *1225*, 15–25.

[66] Stewart, G. W., Hepworth-Jones, B. E., Keen, J. N., Dash, B. C. et al., Isolation of cDNA coding for an ubiquitous membrane protein deficient in high Na+, low K+stomatocytic erythrocytes. *Blood* 1992, *79*, 1593–1601.

[67] Stewart, G. W., Stomatin. *Int. J. Biochem. Cell Biol.* 1997, *29*, 271–274.

[68] Umlauf, E., Csaszar, E., Moertelmaier, M., Schuetz, G. J. et al., Association of stomatin with lipid bodies. *J. Biol. Chem.* 2004, *279*, 23699–23709.

[69] Nawabi, P., Catron, D. M., Haldar, K., Esterification of cholesterol by a type III secretion effector during intracellular *Salmonella* infection. *Mol. Microbiol.* 2008, *68*, 173–185.

